

A Data-Driven Correction of Ultrasonic Source and Receiver Spectral Amplitude Variations

Arno. VOLKER¹, Peter van CAPEL² and Robbert. van VOSSEN¹

¹TNO, Stieltjesweg 1, 2622 KN Delft, The Netherlands

Phone: +31 (0)88 86 66292, e-mail: arno.volker@tno.nl

²University of Utrecht, Julius Institute, Leuvenlaan 4, 3584 CE Utrecht.

Abstract.

The application of phase arrays is growing for NDT applications. State of the art ultrasonic arrays consist of many small piezo-electric elements that can be excited separately to synthesize a desired wave front. This may vary from simple plane waves to complex-shaped focusing wave fields. An implicit requirement is that the source strength (sensitivity) of all elements is equal, to prevent artifacts in the generated wave front. The same holds for the detection of ultrasonic waves. In typical commercial ultrasonic arrays, however, the sensitivity variations can be significant: amplitude variations of ± 3 dB are not uncommon. Pulse-echo data can be used for calibration of element strengths, but has some limitations. Pulse-echo corrections can only be implemented accurately when the sensitivity in transmission is equal to the sensitivity in detection. For ultrasonic measurements this is not necessarily true when separate transmit and receiver arrays are used, but is also not evident when the same array is used. A new data-drive method is demonstrated that can be used to determine the frequency dependent sensitivity of each element in a phase array in emission and detection separately.

Keywords: phase array, ultrasound, inspection, sensitivity correction, inversion,

1 Introduction

Ultrasonic arrays consist of many small piezo-electric elements that can be excited separately to synthesize a desired wave front. This may vary from simple plane waves to complex-shaped focusing wave fields.

An implicit requirement is that the source strength (sensitivity) of all elements is approximately equal, to prevent artifacts in the generated wave front. The same holds for the detection of ultrasonic waves. In typical commercial ultrasonic arrays, however, the sensitivity variations can be significant: amplitude variations of ± 3 dB are not uncommon. Pulse-echo data can be used for calibration of element strengths, but has some limitations. For example, it requires presence of a regularly shaped medium, so that the medium response is equal for all elements. Moreover, pulse-echo corrections can only be implemented accurately when the sensitivity in transmission is equal to the sensitivity in detection. For ultrasonic measurements this is not necessarily true when separate transmit and receiver arrays are used, but is also not evident when the same array is used. The hardware used for the measurement may also play a role here.

In this paper, we present the application of a calibration routine for frequency-dependent emission and recording strengths to ultrasonic transducer elements. The routine, originally developed for the calibration of seismic data, exploits medium reciprocity and uses waveform inversion [1, 2]. A particular advantage is that the calibration can be performed for irregularly shaped media, which can for example even be the medium

under investigation. This allows for a dynamic compensation for varying source and receiver strengths, which can in particular be useful when source and receiver strengths change or deteriorate over time during inspection.

We first discuss the underlying model and its implicit assumptions. For a complete description, we refer to extensive discussions by Van Vossen et al. [1, 2]. The model is then applied to both a synthetic data set, and a set of measurement data obtained in a laboratory setup.

2 Theory

2.1 Initial assumptions

Consider the case where an array is built from N individual ultrasonic source/receiver transducers, located near an arbitrarily shaped reflector. If two separate source/receiver arrays are used, they should be closely spaced. In data collection, all source-receiver combinations are to be fired, recorded and stored separately, leading to N^2 time traces.

For the model to be applied successfully, the sources and receivers should be equally spaced. We furthermore assume that the directivity pattern of each element is approximately equal, and the opening angle is such that for a certain source, a significant amount of receivers is illuminated. Ideally, the transducers should be regarded as point sources. Finally, we assume that the directivity patterns in the out-of-plane direction are approximately equal for all transducers, and reflections returning from out-of-plane events are weak. These conditions are met in most practical applications of ultrasonic arrays, where transducer elements typically have equal dimensions and predominantly two-dimensional structures are under study.

Under these assumptions, variations in recorded signal strength are either caused by varying overall source and receiver strength variations, or a varying medium response. The task at hand now is to extract the correct source and receiver variations.

2.2 Convolutional model in the log-Fourier domain

We describe the recorded signal $V(t)$ by the convolutional equation

$$V(t) = R(t, i) * G(t, j, i) * S(t, j), \quad (1)$$

where, j indicates the source index, i the receiver index, R the i -th receiver response, S the j -th source signal, and G the unknown linear (Green's function) medium response for this source-receiver combination. Here, $(*)$ indicates the convolution operator. By converting to the Fourier (frequency) domain, the $S/R/G$ terms are multiplied rather than convoluted. A more efficient transformation is to the log/Fourier domain:

$$\tilde{V}(\omega) = \log\left(\int V(t) \exp(-i\omega t) dt\right). \quad (2)$$

Then, the measured output for each frequency ω can be expressed as a sum of $S/R/G$ responses rather than a multiplication:

$$\tilde{V}(\omega) = \tilde{R}(\omega, i) + \tilde{G}(\omega, j, i) + \tilde{S}(\omega, j). \quad (3)$$

The real part of $V(\omega)$ corresponds to the signal amplitude, while the imaginary part corresponds to the phase. In the remainder, we restrict the analysis to the real component (limiting the method to amplitude corrections), and neglect varying static phase shifts between the elements.

By transforming to the log/Fourier domain, the problem can now be converted into a system of linear equations [2]:

$$Am(\omega) = d(\omega), \quad (4)$$

where, the data vector $d(\omega)$ contains the measured response at frequency ω , and $m(\omega) = (mG(\omega)^T \ mR(\omega)^T \ mS(\omega)^T)^T$ is the model vector containing the frequency-dependent medium (mG), receiver (mR) and source (mS) response (with T the transpose operator). These vectors have zero average value. In the definition of the matrix A , we have implicitly assumed reciprocity of the medium, $G(t,i,j) = GT(t,j,i)$ [2].

2.3 Regularization criteria

In its current formulation, the solution is underdetermined, that is, there are more unknowns than (linearly independent) equations. We therefore add information to the problem by defining two additional criteria [1], which will be discussed only qualitatively here. The first (I) is that the variation in common-offset sections should be minimal. In other words, when data with common offset is selected from the full set of measurements, the amplitude variations are assumed to be largely caused by source/receiver strength variations. This criterion is valid in case lateral variations (i.e. parallel to the array) in medium structure are weak.

The second criterion (II) is that variations in the common source domain are assumed to be due to variations in source strength, and likewise for receiver strengths in the common receiver domain. In other words, when the energy of all signal strengths received from a single source are summed, the variation with respect to the sum obtained for a different source can be attributed to the variation in source strength. For this criterion to be applicable, a sufficiently large number of receivers should be illuminated by a single source, vice versa.

These criteria provide us with a covariance matrix

$$C_m^{-1} = \begin{pmatrix} C_{mG}^{-1} & 0 & 0 \\ 0 & C_{mR}^{-1} & 0 \\ 0 & 0 & C_{mS}^{-1} \end{pmatrix}, \quad (5)$$

with C_{mG} covariance matrices obtained from quantitatively applying criterion I, and C_{mR} , C_{mS} for criterion II. Though not required, a list of reasonable initial estimates for medium parameters $m_0 = (mG,0(\omega)^T \ mR,0(\omega)^T \ mS,0(\omega)^T)^T$ is obtained as well.

2.4 Inversion

Using the information obtained above, the least-squares solution in the log/Fourier domain is obtained by [3]:

$$m_{LS} = (A^T C_d^{-1} A + C_m^{-1})^{-1} (A^T C_d^{-1} d + C_m^{-1} m_0), \quad (6)$$

where C_d is the (diagonal) data covariance matrix. The source and receiver correction factors in the frequency domain are obtained by calculating $\exp(-mS, LS)$ and $\exp(-mR, LS)$, respectively. Note that in wave synthesis, source corrections should be applied a priori (before source signal emission), while receiver corrections can be implemented a posteriori. The described model is implemented in Matlab. For a typical geometry of 64 elements, an inversion operation for a single frequency component takes several seconds.

3 Applications

We demonstrate our calibration model by considering two examples. The first is a synthetic line array consisting of 64 elements, with source/receiver variations on the full spectrum. The second is a set of experimental data obtained with a 256-element circular array in a laboratory setup.

3.1 Synthetic example

To demonstrate this technology we use a 64 element phase array mounted on a wedge. The wedge is placed on top of a wedge-shaped steel object. This is to show that this method does not require a rectangular test block. This only assumption here is that the back wall should have a smooth shape.

Using finite difference modeling a dataset is generated, where all elements of the array are fired separately (full matrix capture). The signals are recorded by all elements. Random sensitivity variations are introduced in transmission and detection separately. Obviously these variations are consistent with respect to source and receiver.

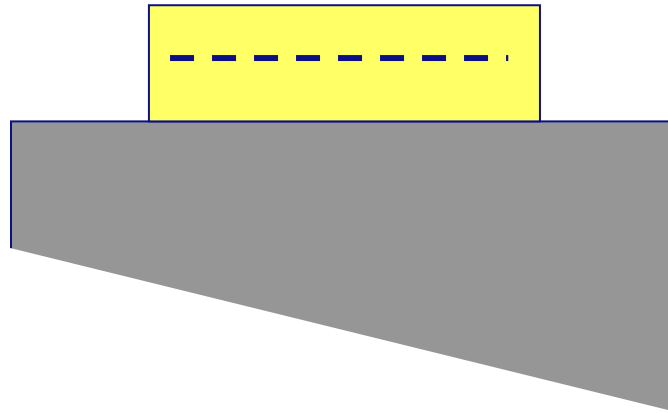


Figure 1. Geometry of numerical example, consisting of a wedge shape steel block and a phase array probe with 64 elements.

A modeled record is shown in Figure 2, before and after applying the random sensitivity variation. For simplicity one scale factor is applied on a time signal, although the method is capable of recovering frequency dependent variations.

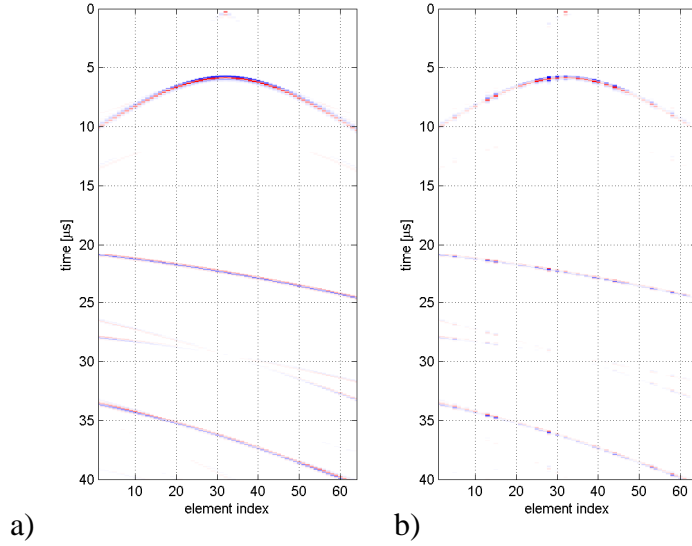


Figure 2. (a) Synthetic model. (b) Typical measured signals.

Running the inversion scheme as described in this paper yields the transmit and receive sensitivities of all elements in the phased array. The inversion result is shown in Figure 3, where the markers indicate the recovered sensitivities and the solid blue line indicates the actual sensitivities. Applying the corrections to the actual sensitivities yields the green line, which is very close to unity. The transmit and receive sensitivities are shown separately.

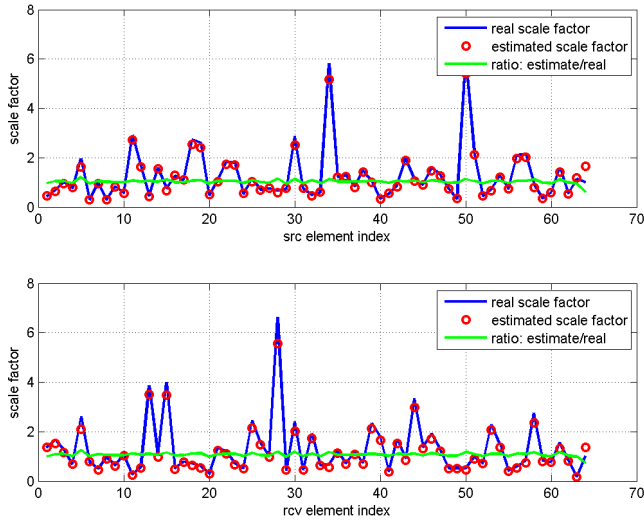


Figure 3. (a) Applied (red) and recovered (blue) source variations. (b) (red) and recovered (blue) receiver variations.

After applying the corrections to the modeled time signals, a very consistent record is obtained. The image quality will greatly benefit from such a high level of consistency. Sensitivity variations are generally known to cause serious artifacts in images.

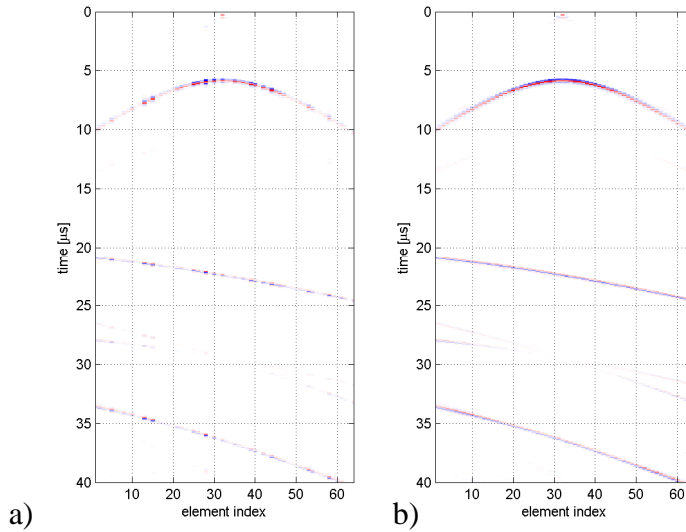


Figure 4 Modeled record with sensitivity variations (a) and after application of corrections for differences in sensitivity in transmission and detection

3.2 Measured data

A picture of the measurement setup is shown in Figure 5. We use a circularly shaped array (7.5" diameter), developed for inspection of oil and gas pipe lines. The array counts 256 source/receiver elements, each of approximately 2 mm diameter and 3 mm height, and emitting at a center frequency of 600 kHz with a typical bandwidth of 100%. For calibration purposes, the array is placed in water in a circular Perspex calibration ring. The 256x256, 100-μs length raw time traces are obtained by multiplexing over all source and receiver channels, and are subsequently pre-amplified and stored digitally. First of all, we look at the pulse-echo data and the integrated signals for each source (defined as the sum of intensities over all receivers, before amplitude correction). Figure 6a shows the pulse-echo signals. Typical variations lie in the range of ± 3 dB, with some elements showing nearly no sensitivity at all. It is known that for one element (index 33), the multiplexer receiver channel is damaged. This means that this element is able to emit, but not receive (something which cannot be derived from pulse-echo data alone).

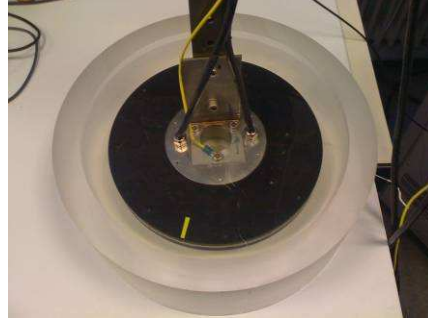


Figure 5. Experimental setup/geometry.

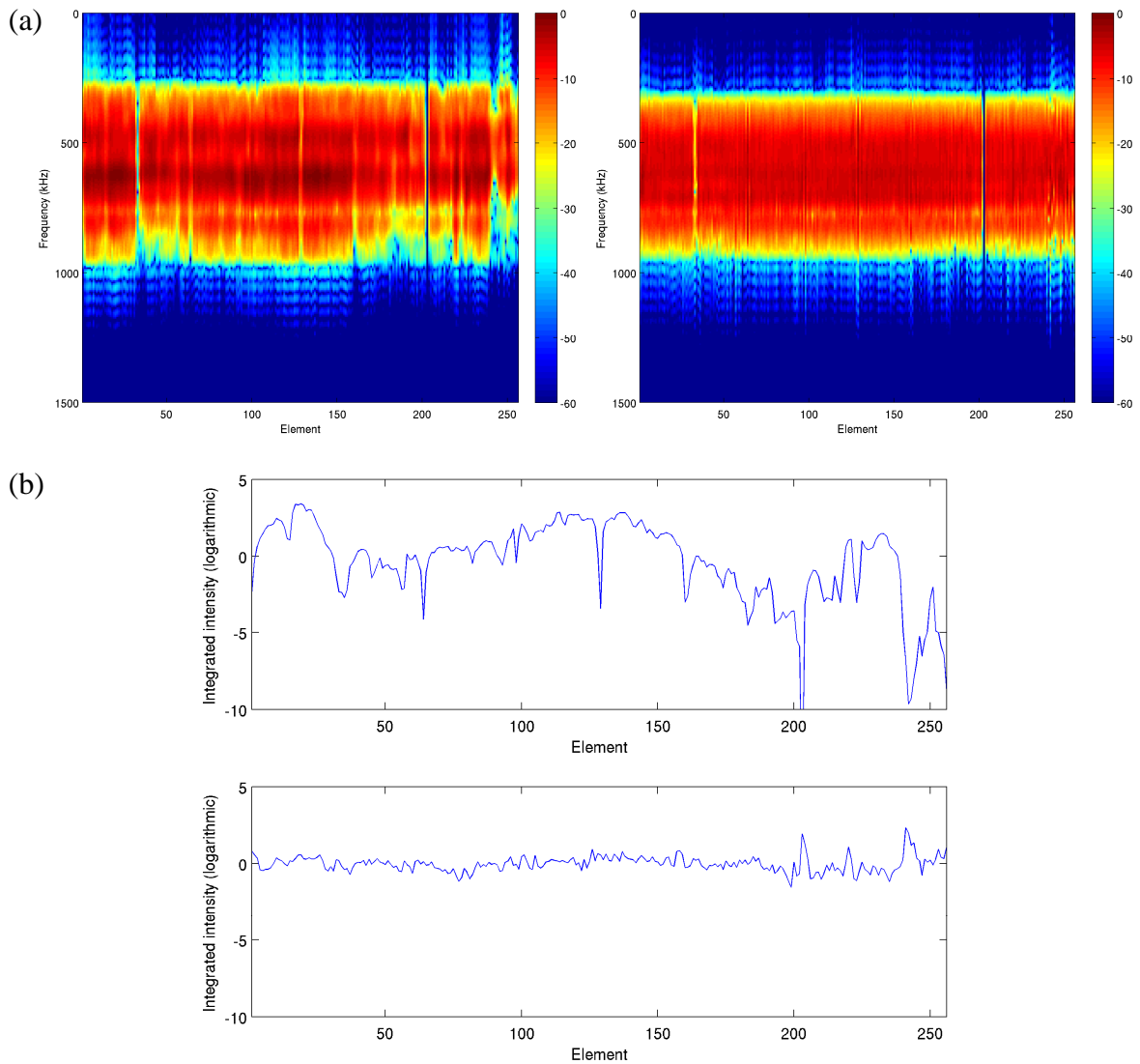


Figure 6. (a) Pulse echo spectral intensities for all elements in the circular array, before (left) and after (right) calibration. Colors indicate spectral intensity in dB. (b) Integrated source intensity variations, before (top panel) and after (bottom panel) calibration.

The source and receiver strengths calculated by the calibration in the range 300-950 kHz are shown in Figure 7. One can see that the intensity variations are larger at the high frequency side (as already demonstrated by Figure 6 a). Specific weak sections (element no. 230 and higher) should be corrected by as much as a factor of six. Over the full array, only small differences between source and receiver correction terms are found, except for the afore-mentioned element 33.

The calibration is now implemented by dividing the frequency-dependent source and receiver strength by the factors shown in Figure 7. The corrected integrated pulse-echo intensities in Figure 6 show a reduction of a factor of five with respect to the uncorrected results, as well as an improved, regularly shaped pulse spectrum.

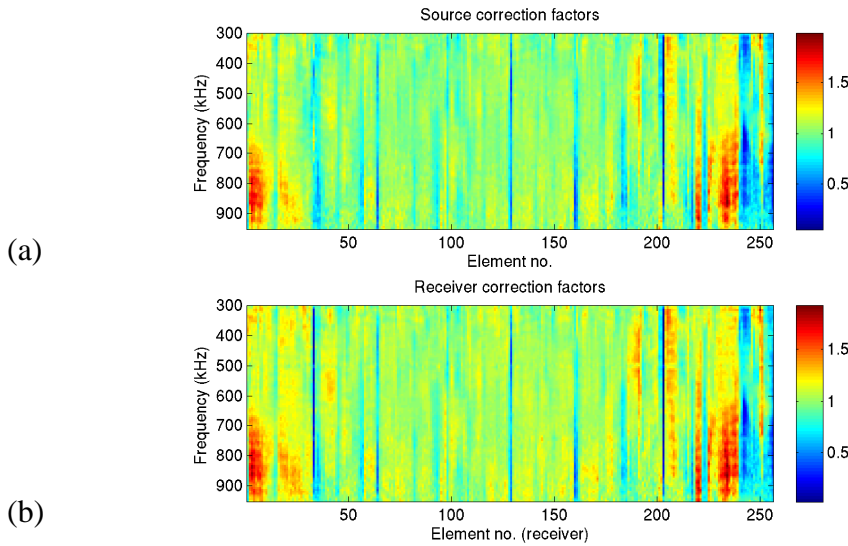
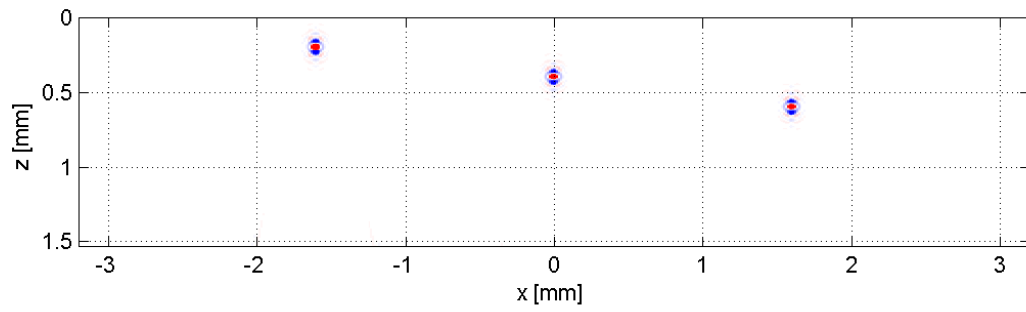


Figure 7. (a) Source strengths determined using the described formalism. (b) Receiver strengths.

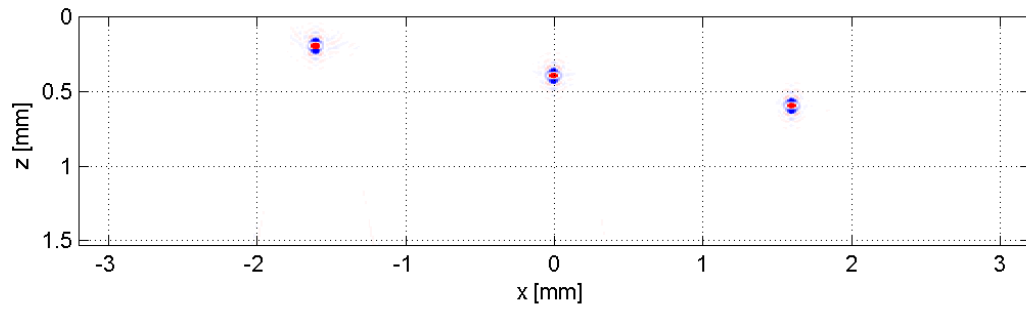
4 Image quality improvement

Sensitivity variations between different elements in a phased array affect the quality of an image. To illustrate this, we modeled the response of three side drilled holes. Amplitude variations were applied to simulate the variation in element sensitivity. The amplitude variations are 1 dB, 3 dB and 6 dB, respectively.

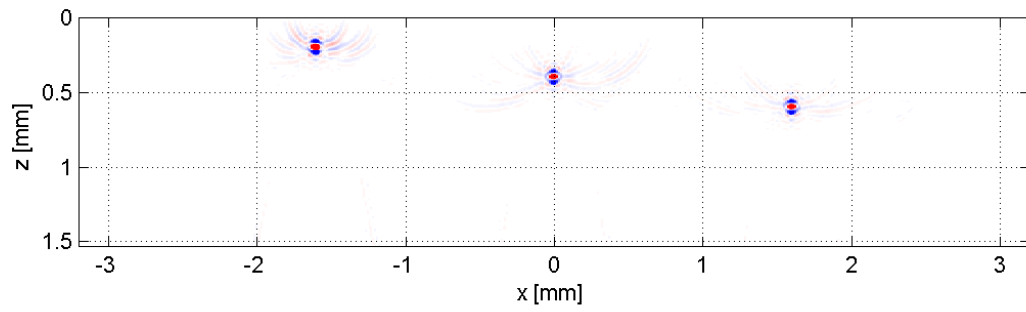
The results are shown in **Figure 8**. The optimal image (no sensitivity variations between the array elements) is shown in **Figure 8a**. Comparison with **Figure 8b**, leads to the conclusion that 1 dB sensitivity variation is quite acceptable since there is no visible degradation of the image. However in case of 3 dB or more (**Figure 8b** and c), the image contains serious artifacts. This effect is more pronounced for the shallow side drilled hole.



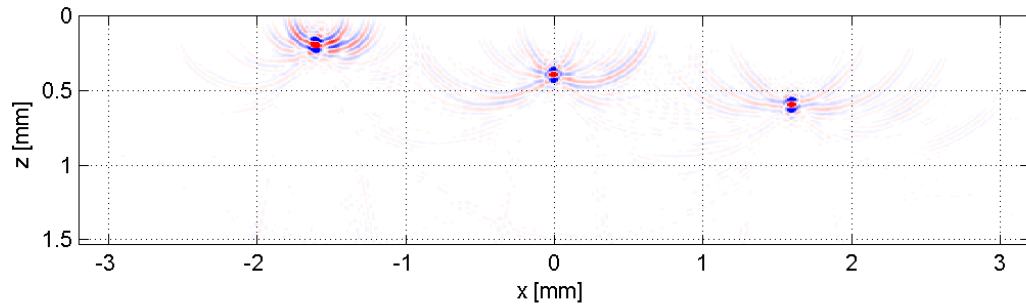
a)



b)



c)



d)

Figure 8 Images of three point diffractors for increasing variation in element sensitivity of the phase array,
a) no sensitivity variation, b) 1 dB variation, c) 3 dB variation, d) 6 dB variation

5 Conclusion

In our view one should try to remove all factors that make inspections component specific. Ultrasonic transducers are known to affect the signal response significantly, reducing the repeatability of measurements.

We have presented a method to correct amplitude variations due to sensitivity variations in elements of ultrasonic arrays. This allows for conditioning of the spectral response of arrays and effectively removing their imprint from the measurement.

This method was demonstrated to yield excellent results on both synthetic and experimentally obtained data. Application of the corrections shows that sensitivity variations can be reduced to less than 1 dB.

Imaging results indicate that 1 dB sensitivity variations are quite acceptable, but the image quality degrades quite quickly if the sensitivity variations are larger than 1 dB. The demonstrated calibration routine can be a valuable tool for various inspection techniques. We are now researching the practical implementation of this method in different array geometries. A next improvement would come from making a correction of static phase shifts for individual elements, which is currently being investigated as well.

References

1. R. van Vossen, "Deconvolution of land seismic data for source and receiver characteristics and near-surface structure", Ph.D. Thesis, Utrecht University (2005).
2. R. van Vossen, A. Curtis, A. Laake and J. Trampart, "Surface-consistent deconvolution using reciprocity and waveform inversion", *Geophysics*, **71**, (2006), pp. V19-V30.
3. A. Tarantola, *Inverse Problem Theory*, Elsevier, Amsterdam (1987).